International Journal of Pharmaceutics: X 5 (2023) 100157

Contents lists available at ScienceDirect

International Journal of Pharmaceutics: X

journal homepage: www.sciencedirect.com/journal/international-journal-of-pharmaceutics-x

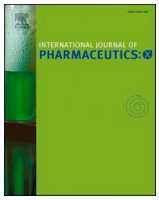

End-to-end approach for the characterization and control of product-related impurities in T cell bispecific antibody preparations

Laurent Larivière [a], Julia Eva Krüger [a], Thomas von Hirschheydt [a], Tilman Schlothauer [a], Katharine Bray-French [b], Martin Bader [a], Valeria Runza [a,*]

[a] Roche Pharmaceutical Research and Early Development, Roche Innovation Center Munich, Penzberg 82377, Germany
[b] Roche Pharmaceutical Research and Early Development, Roche Innovation Center Basel, Basel 4058, Switzerland

ARTICLE INFO

Keywords:
Antibody manufacturing process
Product-related impurities control
Functional characterization
End-to-end approach

ABSTRACT

Antibody-based T cell-activating biologics are promising therapeutic medicines being developed for a number of indications, mainly in the oncology field. Among those, T cell bispecific antibodies are designed to bind one tumor-specific antigen and the T cell receptor at the same time, leading to a robust T cell response against the tumor. Although their unique format and the versatility of the CrossMab technology allows for the generation of safer molecules in an efficient manner, product-related variants cannot be completely avoided. Therefore, it is of extreme importance that both a manufacturing process that limits or depletes product-related impurities, as well as a thorough analytical characterization are in place, starting from the development of the manufacturing cell line until the assessment of potential toxicities. Here, we describe such an end-to-end approach to minimize, quantify and control impurities and -upon their functional characterization- derive specifications that allow for the release of clinical material.

1. Introduction

T cell bispecific (TCB) antibodies are a class of antibody-derived therapeutic proteins that redirect the activity of T cells against tumor cells (Baeuerle and Reinhardt, 2009; Trabolsi et al., 2019; Yu and Wang, 2019). They bind to a cell surface tumor-associated antigen (TAA) on tumor cells and to the T cell receptor (TCR) on T cells, triggering their activation, proliferation, and cytokine release (Bacac et al., 2016a). T cell activation is believed to occur through TCR clustering upon simultaneous binding to both tumor antigen and the CD3 epsilon chain (CD3ε) of the TCR, limiting undesirable activation of T cells in the absence of tumor.

Blinatumomab, the first TCB on the market, has been approved for the treatment of acute lymphocytic leukemia (Franquiz and Short, 2020) and uses the proprietary BiTE™ (Bispecific T cell Engager) format to simultaneously bind CD3ε and CD19 on the surface of target B cells (Einsele et al., 2020). However, due to the absence of an Fc portion, BiTEs have a very short half-life in plasma, limiting their therapeutic applications. Recently, three new TCBs have been approved by health authorities: Tebentafusp-tebn, a soluble TCR directed against gp100 fused to a CD3-binding effector moiety has been marketed for the treatment of uveal melanoma (Dhillon, 2022). Furthermore, two IgG-based TCBs, Mosunetuzumab (CD20/CD3 bispecific), and Teclistamab (BCMA/CD3 bispecific) have been approved for the treatment of follicular lymphoma and multiple myeloma, respectively (Kang, 2022a; Kang, 2022b). Moreover, numerous further second-generation IgG-based TCBs are currently under preclinical or clinical development (Trabolsi et al., 2019; Yu and Wang, 2019).

These molecules vary considerably in their formats and the technology used to ensure correct assembly of the two distinct antigen-binding sites (Brinkmann and Kontermann, 2017). Importantly, and as observed for all antibody-based therapeutics, manufacturing and storage of TCB molecules may generate product-related impurities (Li, 2019) with altered biological activity or impaired pharmacokinetics,

Abbreviations: CE-SDS, capillary electrophoresis-sodium dodecyl sulfate; CRS, cytokine release syndrome; ELISA, enzyme-linked immunosorbent assay; Fc, fragment crystallizable; GMP, good manufacturing process; HIC, hydrophobic interaction chromatography; HMW, high molecular weight (species); IEX, ion exchange chromatography; PBS, phosphate buffer saline; SEC, size-exclusion chromatography; SPR, surface plasmon resonance; TAA, tumor-associated antigen; TCB, T cell bispecific; TCR, T cell receptor.

* Corresponding author.
E-mail address: valeria.runza@roche.com (V. Runza).

https://doi.org/10.1016/j.ijpx.2023.100157
Received 30 September 2022; Received in revised form 23 December 2022; Accepted 1 January 2023
Available online 2 January 2023

that may even be immunogenic, causing undesirable clinical outcomes, such as anaphylaxis or neutralization of the therapeutic protein (Van Beers and Bardor, 2012). Of particular concern are impurities harboring more than a single CD3ε-binding moiety (*e.g.* multimers) due to their ability to activate T cells by TCR multimerization in the absence of target cells (Baeuerle and Reinhardt, 2009; Lee et al., 2019a). During drug discovery and development, emphasis should therefore be put not only on novel designs that limit product-related impurities, but also on the detailed analysis and the set-up of a control strategy to ensure that a product of the required quality will be consistently produced (ICH Harmonised Tripartite Guidelines on Pharmaceutical Development, 2009).

Historically, biotechnological companies have pursued different strategies based on proprietary platforms, which significantly differ from each other. In the present work, we describe a holistic approach to control product-related impurities bearing more than one CD3ε- binding arm, and its application for the assessment of potential toxicities and the definition of clinical-grade specifications. Applied to a [2+1] bispecific monoclonal antibody based on a human IgG1 framework (Bacac et al., 2016b; Lehmann et al., 2016; Bacac et al., 2018) (see Fig. 1a) as a model, this procedure can be extrapolated to many other therapeutic antibodies in development for which similar challenges have to be overcome to ensure product quality and safety.

2. Material and methods

2.1. Generation and selection of a [2+1] TCB producing cell line

CHO-K1-M cells were transfected with the plasmids encoding for the corresponding heavy and light chains of TAA1-TCB in a 1:2 molar ratio, using the Amaxa Nucleofection Kit V (Lonza) and necleofection program U24. For selection of stable transfectants, the cells were transferred to 384-well plates at a cell density of 500 cells/well and cultivated further in the presence of 500 nM methotrexate.

Supernatants were screened by anti-human-Fc ELISA and positive clones were then confirmed by anti-TAA1 and anti-CD3 ELISA (Supplemental Fig. 1). Clonality was achieved later on by serial dilution of clone pools and confirmed by high resolution imaging. Monoclonal cell lines were selected based on a productivity screen (titer) and product quality assays (binding), expanded and deposited as primary seed banks.

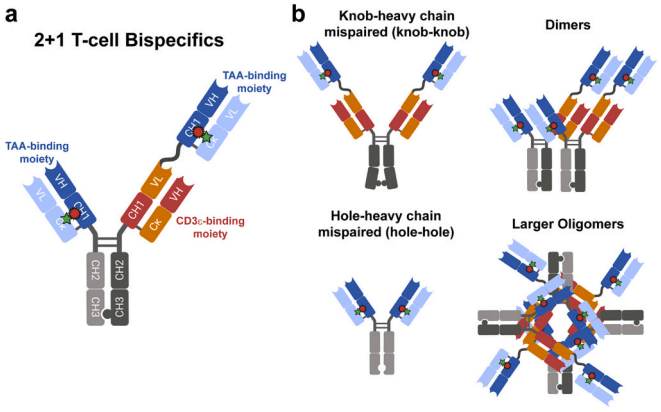

Fig. 1. Formats of TCB monomer and side-products. (a) [2+1] TCB molecular format. The binding to TAA occurs in a bivalent mode to achieve high-avidity on target cells, whereas the binding to CD3ε is monovalent. These molecules have an approximate molecular weight of 200 kDa and comprise two different heavy chains and two different light chains. (b) Possible side-products occurring during manufacturing or storage of [2+1] TCB.

2.2. Micro-purification and analysis of antibodies from culture supernatants

Antibodies were purified from cell culture supernatants by affinity chromatography using MabSelectSuRe-Sepharose™ (GE Healthcare, Sweden). Purification was performed with roboclumns® (Repligen, USA) on a Tecan Evo freedom liquid handling system. Briefly, sterile filtered cell culture supernatants were captured on MabSelectSuRe resin equilibrated with PBS buffer (10 mM Na_2HPO_4, 1 mM KH_2PO_4, 137 mM NaCl and 2.7 mM KCl, pH 7.4), washed with equilibration buffer and eluted with 25 mM citrate, pH 3.0, followed by neutralization with 1 M Tris pH 9.0.

Product quality was analyzed by CE-SDS using LabChip® HT Protein Express Chip and LabChip® GXII protein characterization system (Perkin Elmer) applying the standard protocol for proteins. The identities of the covalent knob-knob and of the "knob-half" impurities were inferred from the comparison of their relative migration time with that of the corresponding isolated impurities (Supplemental Fig. 2).

SEC analysis of Protein A affinity chromatography elution of different clones was performed using a Waters BioSuite 250 HR, 5 µm, 7.8 × 300 mm column. Column was equilibrated with 200 mM KH_2PO_4, 250 mM KCl, pH 7.0. 150 µg TAA1-TCB was injected at a 0.5 mL/min flow rate. The identity of the knob-knob, dimer and larger oligomers impurities were deduced from their elution time, which matched the corresponding isolated species (Supplemental Fig. 3a, bottom panel). The identities of the dimer and knob-knob impurities were further confirmed by SEC - multi-angle light scattering (MALS) analysis, which revealed MWs of approximately 400 kDa and 250 kDa, in accordance with the expected size (data not shown).

2.3. Purification of side-products

For the generation of multimer species, purified product (5 mg/mL) was stressed at 50 °C for 3 weeks in 20 mM histidine, 240 mM sucrose, 10 mM methionine, 0.05% polysorbate 20, pH 5.5. This resulted in an increase of the multimer content to about 5%, as determined by analytical SEC (TOSOH Bioscience TSKgel SuperSW, 4 µm, 7.8 × 300 mm, run isocratically with a 200 mM KH_2PO_4, 250 mM KCl, pH 6.2 buffer). Multimers could be subsequently isolated by tandem SEC. For this purpose, two Superdex® 200 Prep Grade column, 26 mm × 600 mm, were connected in a row, and multimers were eluted isocratically using elution buffer A (20 mM histidine, 140 mM NaCl, pH 6.0). Individual fractions were analyzed by analytical SEC and pooled based on their elution time and purity. Pooled fractions were aliquoted and kept frozen at −70 °C for use in the different assays.

For the isolation of knob-knob and dimer species directly from the process, a cation exchange chromatography side product pool containing low molecular weight species (LMW) and high molecular weight species (HMW) was used. Tandem SEC (two Superdex® 200 Prep Grade columns, 26 mm × 600 mm connected in a row, run isocratically with buffer A) was used as a first step to isolate the different antibody species. Analytical SEC (TOSOH Bioscience TSK gel G3000 SWxl, 5 µm, 7.8 × 300 mm, run with 200 mM KH_2PO_4, 250 mM KCl, pH 7.0) was used to identify the variants contained in each fraction and to define the pooling boundaries. This resulted in different pools. One pool contained almost exclusively dimers and was further polished by SEC (a single Superdex® 200 Prep Grade column, 26 mm × 600 mm, run isocratically with buffer A). Two other pools contained multiple variants and were further processed by tandem SEC (two Superdex® 200 Prep Grade column, 26 mm × 600 mm, connected in a row and run isocratically with buffer A). This in turn resulted in dimer and knob/knob pools. The pools containing one variant were then combined.

For the targeted expression of knob/knob variants, Freestyle HEK 293 cells were transiently co-transfected with three different plasmids encoding the heavy chain containing the "knob" mutations and the two different light chains (1:1:1 ratio). The cells were cultivated in a shaking

flask with F17 as production medium and Feed7, VPA and glucose. Cell culture supernatant was harvested by centrifugation, resulting in a 1.2 L harvest. The knob-knob side-product was first isolated by protein A chromatography, using a column containing 5 mL MabSelect SuRe™ resin. The product was captured from the cell culture supernatant and then washed using three washing steps (step 1: 25 mM Tris/HCl, 25 mM NaCl, pH 7.2, step 2: 0.7 M Tris/HCl, pH 7.2, step 3: 25 mM Tris, 25 mM NaCl, pH 7.2) and eluted with 10 mM acetic acid/NaOH, pH 3.0. For virus inactivation, the sample was incubated for 30 min at room temperature and the pH was then adjusted to pH 5.0 using 1.5 M Tris/HCl. As a second chromatography step, a size exclusion chromatography was performed, using a single Superdex® 200 Prep Grade column, 26 mm × 600 mm, run isocratically with buffer A. Cation exchange chromatography (Poros®XS column, 8 mm × 20 mm) was used as last chromatography step. The column was equilibrated with 35 mM acetic acid/NaOH, pH 5.0 and the knob-knob side-product was eluted using a 0–100% 35 mM acetic acid/NaOH, 1 M NaCl gradient. The content of knob/knob fragments in each fraction was determined by analytical SEC (TOSOH Bioscience TSK gel G3000 SWxl, 5 µm, 7.8 × 300 mm, run with 200 mM KH_2PO_4, 250 mM KCl, pH 7.0). Fractions containing the knob/knob species with purity ≥97% were pooled.

2.4. Evaluation of analytical chromatography and electrophoresis methods for control of HMW variants

All chromatographic analyses of spiked samples were performed using an HPLC system equipped with data acquisition software. Elution was monitored by measuring optical density at 280 nm.

For IEX, samples were injected onto a MAbPac SCX-10, BioLC, 4 × 250 mm column (Thermo Fisher) equilibrated with low pH buffer (CX-1 pH Gradient Buffer pH 5.6, Thermo Fisher) and eluted using a gradient of high pH buffer (CX-1 pH Gradient Buffer, pH 10.2, Thermo Fisher).

For HIC, samples were injected onto a TSKGel Ether-5PW column (7.5 × 75 mm, 10 µm, Tosoh Bioscience) equilibrated with high salt buffer (25 mM sodium phosphate. 1.5 M ammonium sulfate, pH 7.0) and eluted using a gradient of low salt buffer (25 mM sodium phosphate, pH 7.0).

For SEC, performance of two different SEC columns were compared (Waters BioSuite 250 HR, 5 µm, 7.8 × 300 mm, 5 µm and Tosoh Bioscience TSKgel SuperSW mAb HR, 7.8 × 300 mm, 4 µm). Columns were equilibrated with 200 mM KH_2PO_4, 250 mM KCl, pH 7.0. 150 µg TAA1-TCB was injected at a 0.5 mL/min flow rate.

Electrophoretic analysis of spiked samples were performed on a capillary electrophoresis system (Beckmann) mounted with an 21-cm uncoated fused-silica capillary (50-µm ID). Samples were labeled with 3-(2-furoyl) quinoline-2-carboxaldehyde using standard procedures. After 30 s (reduced samples) or 40 s (non-reduced samples) injection through applying a 5 kV voltage, separation was performed by applying a 15 kV voltage. Detection was performed using an argon-ion laser (excitation at 488 nm, emission at 600 nm (± 20 nm)).

2.5. Surface plasmon resonance

All SPR Biacore T200 experiments were carried out in HBS-P+ pH 7.4 running buffer (GE Healthcare) and at 25 °C. SA-chips (GE Healthcare) were coated with the biotinylated target (1 µg/mL solution of target in HBS-P+). To determine the kinetic profile TCB samples were diluted with HBS-EP+, pH 7.4 buffer to a concentration of 600 nM and then serially diluted with a running buffer in 1:3 ratio to 200 nM, 67 nM, 22 nM and 7 nM. All sample dilutions were analyzed using 120 s association time at a flow rate of 60 µL/min. The dissociation time of 600 nM and 200 nM sample dilutions was monitored for 720 s at a flow rate of 60 µL/min. The surface regeneration was performed by a 60 s washing step with a 10 mM glycine pH 2.1. Binding curves were evaluated using the Biacore T200 BIAevaluation software version 3.1, and for the calculation of binding properties 1:1 Langmuir binding model was used. Further analysis of heterogeneous interaction was performed using Interaction Map software (TraceDrawer, Ridgeview Instruments AB).

2.6. Cell lines

Jurkat NFAT-luc acute lymphatic leukemia cell line, expressing a luciferase reporter under the control of an NFAT-dependent promoter was purchased from Promega Corporation. Cells were cultured in RPMI medium with HEPES, GlutaMAX, MEM NEAA, Sodium pyruvate, 10% fetal calf serum (FCS) and 200 µg/mL hygromycin B. The target cell line was purchased from ATCC and cultured in IMDM with HEPES, L-glutamine and 10% FCS. A549 lung carcinoma cell line was generated in-house by lentiviral transduction with human full length TAA2. Cells were cultured in DMEM with high glucose, L-glutamine, pyruvate, 10% FCS and 4 µg/mL Puromycin dihydrochloride. All cells were passaged twice a week.

2.7. Cell-based assays

For TAA1-TCB, eight protein sample dilutions from 12 µg/mL to 0.46 pg/mL were prepared in test medium, consisting of RPMI medium with HEPES, GlutaMAX, MEM NEAA, Sodium pyruvate and 10% FCS supplemented with Penicillin Streptomycin. 50 µL of antibody solution was added to the wells of white 96 well plates. To analyze target-dependent T cell activation (TDA), 50 µL of a 1 to 1 mixture of target cells and Jurkat NFAT-luc effector cells at a total cell number of 4×10^4 in test medium was added to each well. To analyze target-independent T cell activation (TIA), only 50 µL of Jurkat NFAT-luc effector cells in test medium at a total cell number of 2×10^4 were added to each well. The assay plates were incubated for 4.75 h in an incubator at 37 °C and 5% CO2 and equilibrated to room temperature for 15 min. 100 µL of Steady-Glo (Promega) bioluminescence readout reagent was added to each well. Plates were shaken for 30 min at room temperature before bioluminescence readout using a microplate reader (SpectraMax L, Molecular Devices).

For TAA2-TCB, eight protein sample dilutions from 10 µg/mL to 97.66 pg/mL were prepared in test medium, consisting of RPMI medium with HEPES, GlutaMAX and 10% FCS supplemented with Gentamicin. 50 µL of antibody solution was added to the wells of white 96 well plates. To analyze target-dependent T cell activation (TDA), 50 µL of a 1 to 2 mixture of A549 target cells and Jurkat NFAT-luc effector cells at a total cell number of 6×10^4 in test medium was added to each well. To analyze target-independent T cell activation (TIA), only 50 µL of Jurkat NFAT-luc effector cells in test medium at a total cell number of 4×10^4 were added to each well. The assay plates were incubated for 2.75 h in an incubator at 37 °C and 5% CO2 and equilibrated to room temperature for 15 min. 100 µL of ONE-Glo Ex (Promega) bioluminescence readout reagent was added to each well. Plates were shaken for approximately 10 min at room temperature before bioluminescence readout using a microplate reader (SpectraMax L, Molecular Devices).

Each concentration was tested in duplicate on one plate. The relative luminescence units (RLU) of duplicates was averaged. The dose-response curves are generated by plotting the RLU against the concentration of the antibody preparation (x-axis) using a 4-parameter logistic fit, model 201 (XLfit, idbs). In order to enable comparability of all TAA1-TCB and TAA2-TCB samples, all sample curves from the TDA- and TIA assay were normalized to the respective TAA1- and TAA2-TCB monomer curves in the TDA assay according to the formula:

(RLU Value SAMPLE – Lower Asymptote MONOMER CURVE TDA) / (Higher Asymptote MONOMER CURVE TDA – Lower Asymptote MONOMER CURVE TDA) * 100 = Normalized Activity [%].

2.8. Whole blood assay

Venous blood from 6 healthy blood donors was collected in vacutainer tubes with lithium heparin as anticoagulant and kept at room

temperature until initiation of the assay which was within 3 h of blood withdrawal.

195 µL of whole blood was added to test items in triplicate in round bottom 96 wells plates followed by incubation at 37 °C with 5% CO2 for 24 h. Cells and plasma were separated by centrifugation at 1800 *g* for 5 min and plasma samples were stored at −80 °C until analysis of cytokine content. After plasma collection, 70 µL PBS was added to each well and triplicates pooled for flow cytometry.

2.9. Cytokine analysis

Plasma samples were diluted 1 to 10 and analyte concentrations were determined by ELISA using the Human Cytokine chemiluminescent Assay Kit (Aushon SearchLight, Cat. No 84619B) with the SignaturePLUS™ imaging system and the Cirasoft™ Analysis Software. Reconstitution volumes of standards were adapted to extend the standard curve as follows: IFNg, 500 pg/mL; IL-1a, 1800 pg/mL; IL-1ß, 200 pg/mL; IL-2, 320 pg/mL; IL-6, 2000 pg/mL; IL-8, 4000 pg/mL; IL-10, 200 pg/mL; IL-12p70, 1200 pg/mL; TNFa, 1000 pg/mL. Shown data represent the mean of cytokine measurements in supernatants from triplicate wells. Data for IL-12, and IL-1a were below the lower limit of quantification in monomer alone samples from 3 out of 6 donors, and were not included in the analysis.

2.10. Expression of CD69 on CD4+ T cell subsets

Following treatment of whole blood with antibody, triplicate samples were pooled and 50 µL of cells were stained with anti-CD45 BV510 (clone HI30, BIOLEGEND#304036), anti-CD3 APerCPCy5.5 (clone UCHT1, BIOLEGEND#300430), anti-CD4 V450 (clone RPA-T4, BD#560343), anti-CD8 APCCY7 (clone SK1, BL#344714), anti-CD69 FITC (clone FN50, BIOLEGEND#310904, Lot#2230656), isotype control FITC (clone MOPC-21, BD#555748, Lot#28391) for 30 min at room temperature. After washing, erythrocytes were lysed with pharmlyse buffer BD#555899. Cells were then washed and resuspended. Data were acquired on a BD Canto II flow cytometer and analyzed using FlowJo software (Trestar). A student's *t*-test was used to test for statistically significant increases compared to the TAA1-TCB monomer.

3. Results

3.1. Optimal molecule design, cell line and purification process

The [2+1] TCB molecule described here is directed against a tumor-associated antigen, TAA1, and will thereafter be referred to as TAA1-TCB (Fig. 1a). Its design is based on the CrossMab technology to ensure proper pairing of the different heavy and light chains (Klein et al., 2019; Regula et al., 2018).

Despite “knob-into-hole” mutations, low level of heavy chain homodimerization can occur, generating improperly assembled “hole-hole” and “knob-knob” impurities (Carter, 2001; Kuglstatter et al., 2017) (Fig. 1b). In our experience, co-transfected mammalian cells are more prone to produce hole-hole impurities than knob-knob impurities. Therefore, to limit the amount of side-products able to bind CD3ε bivalently, “knob” mutations are introduced in the heavy chain harboring the CD3ε-binding moiety and “hole” mutations in the heavy chain containing the TAA1 binding moiety only (Fig. 1a). The resulting knob-knob homodimer could bind to both CD3ε as well as the TAA1 in a bivalent manner, and has an approximate molecular weight (MW) of 250 kDa, whereas the 150 kDa hole-hole homodimer can bind to TAA1 only (Fig. 1b). In addition to knob-knob impurities, molecule aggregates could also potentially crosslink the TCR through multivalent CD3ε binding. In this study, we distinguish between dimers and larger oligomers (Fig. 1b). While dimers have an approximate MW of 400 kDa, larger oligomers exceed 600 kDa. Altogether, all of these high molecular weight (HMW) species could potentially activate T cells in the absence of tumor target cells.

[2+1] TCB molecules can be easily expressed and properly assembled in single mammalian cell lines co-transfected with genes coding for the four different chains, and with yields, stability and quality comparable to natural IgG antibodies (Klein et al., 2019). For the production of biologics for clinical trial and market supply purposes, the cell line is usually generated by stable transfection followed by subcloning steps to ensure clonality (Lalonde and Durocher, 2017; ICH Harmonised Tripartite Guideline on Quality of Biotechnological Products Q5D, 1997). Although product-related impurities may be efficiently removed during downstream processing, an approach limiting the amount of impurities initially present in cell culture supernatants is highly desirable. This is especially relevant in the present case due to the complex side-product profile related to the format. Indeed, separation of side-products usually comes at the cost of purification yield. Furthermore, depending on the differences regarding biochemical and biophysical properties between the desired product and its impurities, separation using standard chromatography techniques may be challenging. Accordingly, a significant effort was made to ensure the selection of a cell clone producing the lowest levels possible of product-related impurities, paying special attention to HMW species. In addition, clone stability with regards to side-product profile upon cell aging was of fundamental importance. In comparison to standard antibodies, a more detailed and earlier characterization of a larger number of clones was therefore necessary to identify a suitable manufacturing cell line. Following subcloning and re-testing, approximately 100 clones were selected based on their expression titers and target-binding profiles, as determined by ELISA. Their supernatants were micro-purified and further characterized regarding their product quality by capillary electrophoresis - sodium dodecyl sulfate (CE-SDS, Fig. 2a) and analytical size-exclusion chromatography (SEC, Fig. 2b). Besides the main product, the profiles exhibit additional components. Here, the term “knob-half” refers to a side-product formed by the “knob”-mutated heavy chain and both TAA- and CD3-binding light chains. Interestingly, levels of the covalent knob-knob impurities measured by non-reducing CE-SDS were very low for all clones, and could not account for the total levels of knob-knob observed by analytical SEC. On the other hand, the amounts of knob-halves in CE-SDS and knob-knob impurities in analytical SEC correlated well. Therefore, we concluded that most knob-knob impurities expressed by these clones consist of non-covalently associated knob-halves species. This finding may be explained by an alternative arrangement of the CH2 and CH3 domains, which precludes pairing of the cysteines normally involved in the canonical intermolecular disulfide bonds (Elliott et al., 2014).

Based on these results and the potential of HMW species to activate T cells in a target independent manner, the levels of HMWs and knob-halves were used as one of the main criteria for manufacturing cell line selection. Fig. 2c summarizes the results of the analytical characterization of the 114 clones under consideration. Although a large portion of them exhibited levels of knob-knob impurities below 5%, they significantly differed in their knob-knob content, ranging from <1% up to >35%. Clones with low levels of knob-knob (<5%) greatly varied in their hole-hole content (Fig. 2c, lower panel). Interestingly, high levels of knob-knob and hole-hole seemed mutually exclusive, supporting the hypothesis that the product quality is driven by the correct balance of expression of the two heavy chains (Li, 2019). The final selected clone features a low level of knob-knob and overall HMW impurities (< 1% and ≤ 3%, respectively) after Protein A affinity chromatography, > 80% main product content and an acceptable titer (1.8 g/L culture). Also, the final clone shows an excellent stability of the product quality profile over time (data not shown).

The next step towards a production process to support clinical studies was to establish a suitable downstream processing. Unlike other known approaches for the purification of bispecific molecules that rely on the cumbersome *in vitro* assembly of the final product (Giese et al., 2018; Labrijn et al., 2013), the IgG-like properties of the TCB described

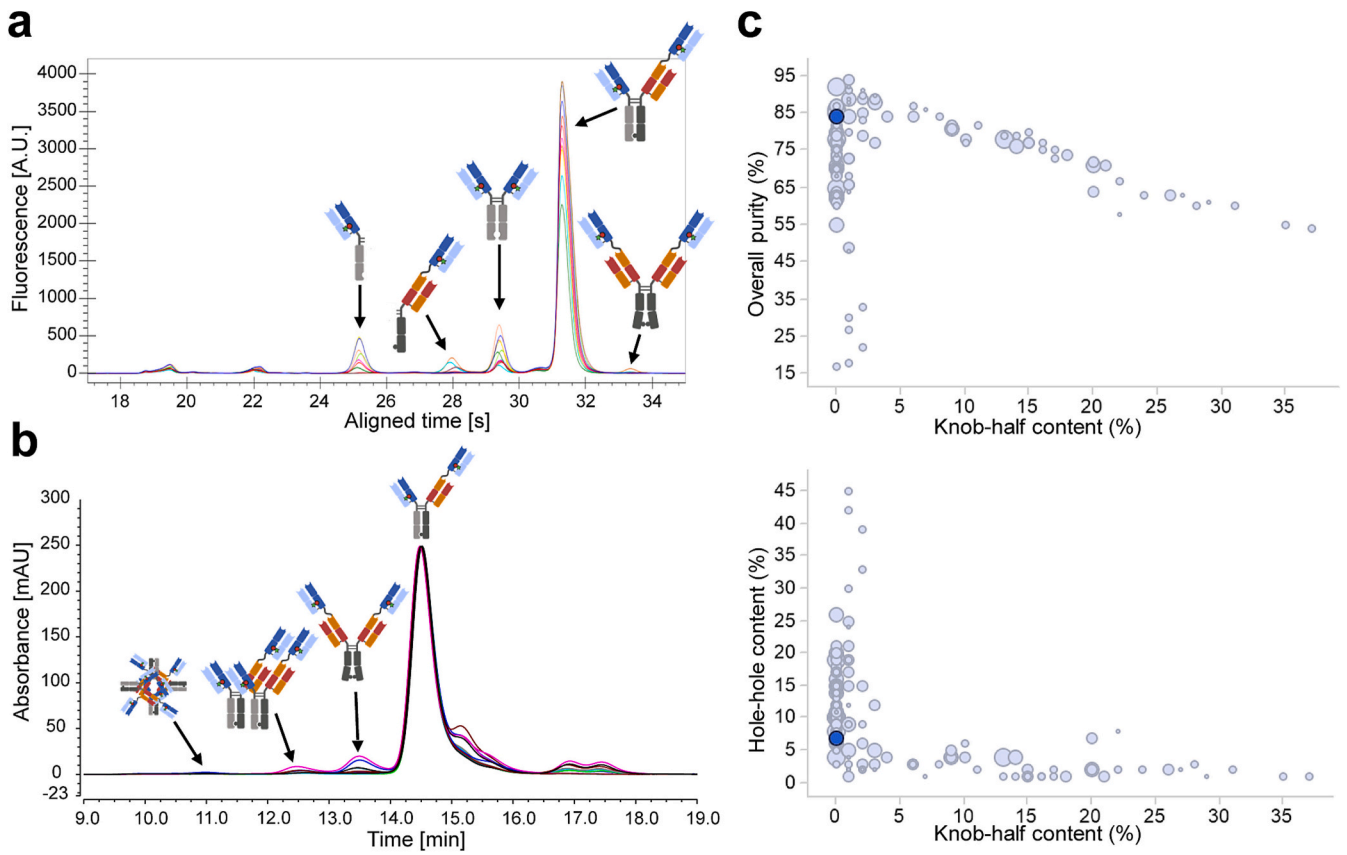

Fig. 2. Side-product profile of selected TCB expressing clones upon Protein A affinity chromatography elution. (a) Non-reducing CE-SDS analysis. The identity of the components was deduced from their theoretical MW under non-reducing and reducing conditions. (b) SEC analysis. Intensities were normalized to the main peak for clarity. (c) Purity and side-product content analysis of 114 clones, as determined by non-reducing CE-SDS. The size of the corresponding dots is proportional to the product titer. The selected manufacturing cell line is indicated in dark blue. (For interpretation of the references to colour in this figure legend, the reader is referred to the web version of this article.)

here, together with the quality of the supernatant, allowed for a generic 3-column process to obtain clinical-grade material (Supplemental Fig. 4a). Protein A affinity chromatography removed media components, product-related impurities lacking an Fc part and host cell proteins, while cation exchange chromatography allowed for depletion of remaining amounts of other product-related impurities, including HMW species (knob-knob, dimers and larger oligomers, Supplemental Fig. 4b). Finally, anion exchange chromatography was used to remove residual host cell DNA and virus-like particles.

Due to the ability of the cation exchange chromatography to separate HMW species from the desired product, it was possible to fine-tune their percentage in the final material by adjusting the pooling limits. This enabled, in turn, to produce material for toxicological studies with higher HMW amounts compared to clinical batches, thereby contributing to the toxicological assessment of these potentially safety-relevant species (Supplemental Fig. 4b).

In order to develop proper methods to control the levels and functionality of HMW species, the different molecular species were purified to homogeneity. For this purpose, two strategies were followed (Supplemental Fig. 3). In the first approach, stressed material as well as a pool of fractions derived from the cation exchange chromatographic purification step (Supplemental Fig. 3a, top panel), which contained a mixture of the previously mentioned impurities in significant amounts, were subjected to preparative SEC. Due to their different molecular weights, the individual impurities elute at different time points and can be efficiently separated. Analytical SEC and CE-SDS analysis of the purified product-related variants confirmed that they mainly contained the desired side-products (Supplemental Fig. 3a, bottom panel and data not show). This strategy, though efficient, may not be generalizable to all types of format-specific T cell activating impurities since the purification for knob-knob variants relied on its larger size in comparison to the main product, which is specific for the [2+1] format. In addition, large amounts (>1 g) of starting material were necessary to obtain a few milligrams of purified variants, since the impurities only constitute a minor fraction of the starting material. Significant amounts are often only available at a later stage of technical development, whereas purified variants should be available as early as possible to support method development and toxicological assessment. For this reason, we devised an alternative approach for the targeted expression of knob-knob impurities. HEK cells were transiently co-transfected with the genes coding for the heavy chain containing the “knob” mutations and the two different light chains. In the absence of the genes coding for the heavy chain containing the “hole” mutations, no properly assembled molecules can be produced. Indeed, analysis of the material obtained after protein A purification (Supplemental Fig. 3b, top panel) revealed that the cells mainly produced a mixture of half-antibodies and the desired knob-knob variant. The latter species could be further purified to homogeneity by preparative SEC (Supplemental Fig. 3b, bottom panel). In contrast to the previous method, this approach only required a medium-scale expression (1 L) to obtain milligrams of the purified knob-knob variant.

3.2. Tailored-made control method for precise and robust quantification of HMW species

Despite careful selection of the producing cell line and the development of a downstream process ensuring an efficient depletion of the remaining side-products, low levels of HMW species are still present in the final purified material, which should be properly controlled by one

or more analytical methods (ICH Harmonised Tripartite Guideline on Specifications Q6B, 1999). Especially, in cases where different HMW species show different biological activities, the chosen approach should be able to discriminate between them. Moreover, the methods should be sensitive enough to detect impurity levels below 1%, and finally be highly reproducible and implementable in a GMP environment. Based on previous experiences, hydrophobic interaction chromatography (HIC), ion exchange chromatography (IEX), CE-SDS, and SEC profiles were considered, and the profiles of purified knob-knob and dimer variants were compared with the corresponding profiles of the purified product.

Analytical HIC revealed two distinct main peaks for both isolated knob-knob and dimer impurities, revealing that they contain different subpopulations (Fig. 3a). Whereas both dimer peaks elute at significantly different times, the knob-knob impurity partially co-elutes with the purified product, making the method not suitable for monitoring this impurity.

For analytical IEX, both impurities clearly show main peaks which elute later than the desired product (Fig. 3b). Nevertheless, the usefulness of IEX for reliable quantification of impurities was limited due to the complex charge pattern, with the main peak representing only a part of the total peak area. This is not surprising since dimers and knob-knob impurities can also exhibit further heterogeneities like deamidation, N- or C-terminal modifications, which affect their charge. Accurate quantification would require summation of all peaks, which is practically not possible since some charge variants of the impurities may overlap with charge variants of the main product.

Non-reducing CE-SDS was originally used to monitor knob-knob impurities during cell line development and appeared to be a promising approach. We performed spiking experiments with isolated knob-knob into the purified product prior to CE-SDS analysis to determine the relative migration time of this variant. As expected, two new peaks were observed, corresponding to the covalent and non-covalent knob-knob species (Fig. 3c). Whereas the non-covalent version was clearly separated from the main product, the covalent version migrated within the tail of the main product peak, rendering the method not suitable. Furthermore, reproducibility and recovery were not sufficient to ensure an accurate quantification under 1% (Fig. 3c). Finally, analysis of stressed material showed an increase in the intensity of the peak corresponding to the non-covalent variant. Since no change in the knob-knob content is expected upon stress, we concluded that fragments with similar size co-migrate with the non-covalent variants. Therefore, using CE-SDS as a quantification method would potentially lead to an overestimation of the knob-knob impurities.

Finally, SEC was used to monitor HMW species during cell line development and proved to detect all of them. Additionally, SEC is known to generally offer good sensitivity and reproducibility for controlling HMW species (Hong et al., 2012). The challenge in this specific case consisted in the proper separation of the knob-knob impurities, which differ from the main product by only 50 kDa. After careful evaluation, the Tosoh TSKgel SuperSW column proved to be the best option: knob-knob amounts as low as 0.1% could be clearly detected and separated from the main peak, allowing for consistent and reproducible quantification down to 0.2% (Fig. 3d). Furthermore, separation from dimers was sufficient to enable quantification of different HMW variants. Finally, this method was validated and implemented in a GMP environment for the control of HMW species in clinical batches.

3.3. *Functional characterization of HMW species confirms their target independent-mediated T cell activity potential*

The biological activity of the different purified HMW species was investigated *in vitro*. In a first step, we verified by surface plasmon resonance (SPR) whether the variants were able to bind CD3 in a multivalent manner (Supplemental Fig. 5). The Fc-fused CD3δ/ε extracellular domains were immobilized on a sensor chip and interactions with the different TCB side-products were analyzed (Supplemental Fig. 5a). Whereas the monomer shows a relatively fast dissociation half-life of about 3 min, all HMW species displayed a slower dissociation (> 60 min). This is a clear indication for avid binding to CD3δ/ε, which in turn points at the ability of HMW species to bind CD3ε mutivalently. Similarly, we analyzed the valency of the interaction between the variants and their TAA target (Supplemental Fig. 5b). In contrast to its CD3 counterpart, interaction of the TAA1-TCB monomer with TAA can be bivalent. This explains the observed biphasic curve, with a fast dissociation corresponding to the monovalent binding followed by a slow dissociation due to the bivalent binding. The different HMW variants show a similar behavior with the ratio between slow and fast

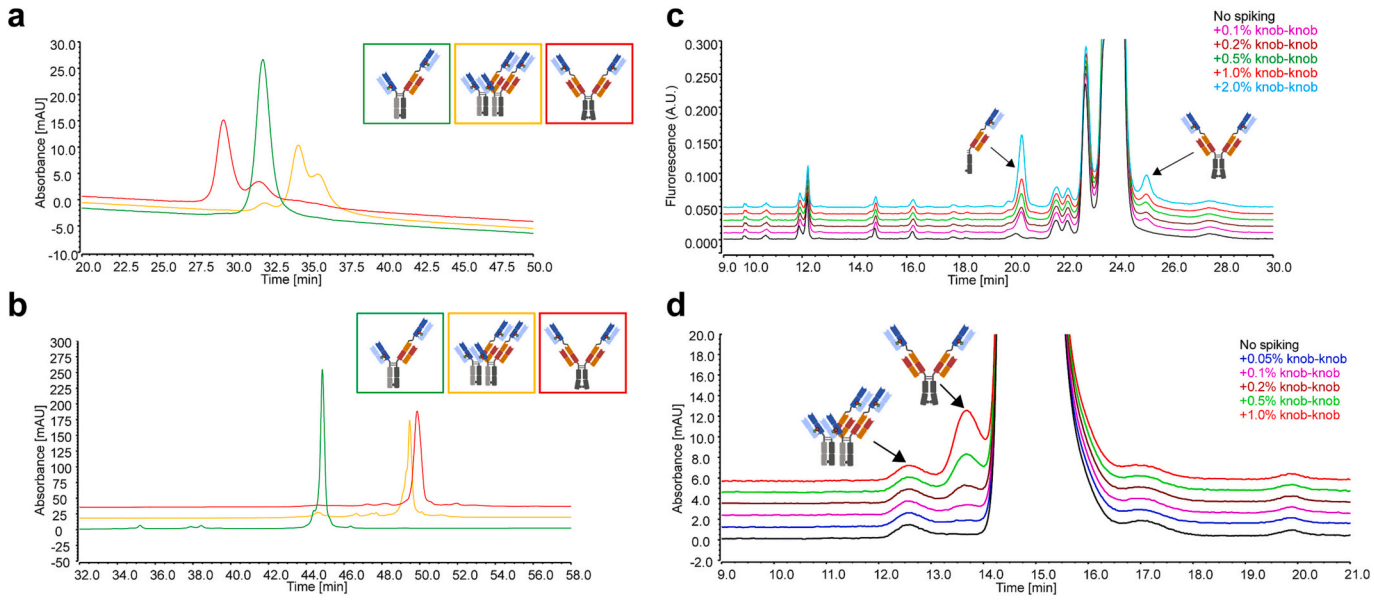

Fig. 3. Evaluation of different methods for the quantification of HMW species. (a-b) Elution profile of the TAA1-TCB main product and the corresponding isolated dimer and knob-knob after (a) analytical HIC, and (b) analytical IEX. (c-d) Electrophoretic and chromatographic elution profile of purified TAA1-TCB spiked with various amounts of purified knob-knob side-products after (c) CE-SDS and (d) analytical SEC. For the analytical SEC, a Tosoh Bioscience TSKgel SuperSW mAb HR column was used.

dissociation being increased, illustrating their higher ability for TAA multimerization (Supplemental Fig. 5). In a second step, different TAA1-TCB samples were analyzed in a cell-based reporter gene assay (Stecha et al., 2015). Briefly, TAA1-TCB can bind TAA1 expressed on the surface of tumor cells and to surface-exposed CD3 on T cells (Jurkat NFAT-luc, Fig. 4a). T cell activation occurs then only upon simultaneous binding of the TCB to both targets, due to TCR clustering. Subsequent downstream signaling pathways activate the transcription factor NFAT that promotes expression of an NFAT-dependent luciferase reporter, which can be monitored by measuring bioluminescence. Recently, Lee et al. reported a similar assay using an NFκB response element and demonstrated that it correctly reflects the mode of action (Lee et al., 2019a).

In the target-dependent assay, TAA1-TCB monomer showed the expected dose-dependent activity with a single-digit picomolar EC50, reflecting the high potency of the molecule (Fig. 4c). The isolated knob-knob and dimer variants also exhibited significant activities, though slightly reduced, whereas the larger oligomers were inactive (Fig. 4c). In this setting, the observed higher valency for CD3 and TAA interactions did not translate into an increased potency, suggesting a suboptimal molecular geometry of the impurities.

In order to investigate the potential of the HMW variants to activate T cells in a TAA-independent manner, we performed the same assay in the absence of target cells (Fig. 4b). As expected, the purified TAA1-TCB did not show any activity, even at concentrations above 10 μg/mL (Fig. 4d). In contrast, the isolated knob-knob and dimers showed some limited activity (Fig. 4d and e), however, at concentrations about 1000-fold higher than the amounts required to induce a robust target-dependent T cell activation by the TAA1-TCB monomer. Bivalent CD3 binding in *cis* is therefore able to trigger TCR multimerization and T cell activation, although to a much lower extent than crosslinking *in trans*.

Since the TCB potency can strongly depend on the TAA and its copy number (Ellerman, 2019), we investigated target-dependent and -independent T cell activation for another [2+1] TCB, namely TAA2-TCB, and its isolated HMW variants. TAA2-TCB exhibits dose-dependent potency in the presence of cells expressing TAA2, with an EC50 about 50-fold higher than TAA1-TCB (Fig. 4f). Like TAA1-TCB, TAA2-TCB was not active in the absence of target cells (Fig. 4g and h). TAA2-TCB knob-knob and dimers activated T cells in a target-independent manner, although the former triggered T cell activation at significantly lower concentrations than the latter (Fig. 4g and h). This suggests that both TCBs knob-knob and dimer variants lead to a comparable though distinct TCR clustering through bivalent CD3 binding. As expected, TAA2-TCB knob-knob and dimers also showed activity in the presence of target cells that is even higher than that of the monomer (Fig. 4f). A possible explanation for this difference with TAA1-TCB may be the lower potency of the monomer. Indeed, in the case of TAA2-TCB variants, TCR dimerization mediated by bivalent CD3 binding *in cis* may synergize the TCR clustering mediated by TAA2 binding *in trans*. Finally, in contrast to TAA1-TCB, larger oligomers were able to activate T cells, both in a target-dependent as well as independent fashion, although at higher concentrations than the knob-knob and dimer variants. The discrepancy between both TCBs in this respect might be explained by structural differences, since antibody oligomers are known to be heterogeneous species (Roberts, 2014).

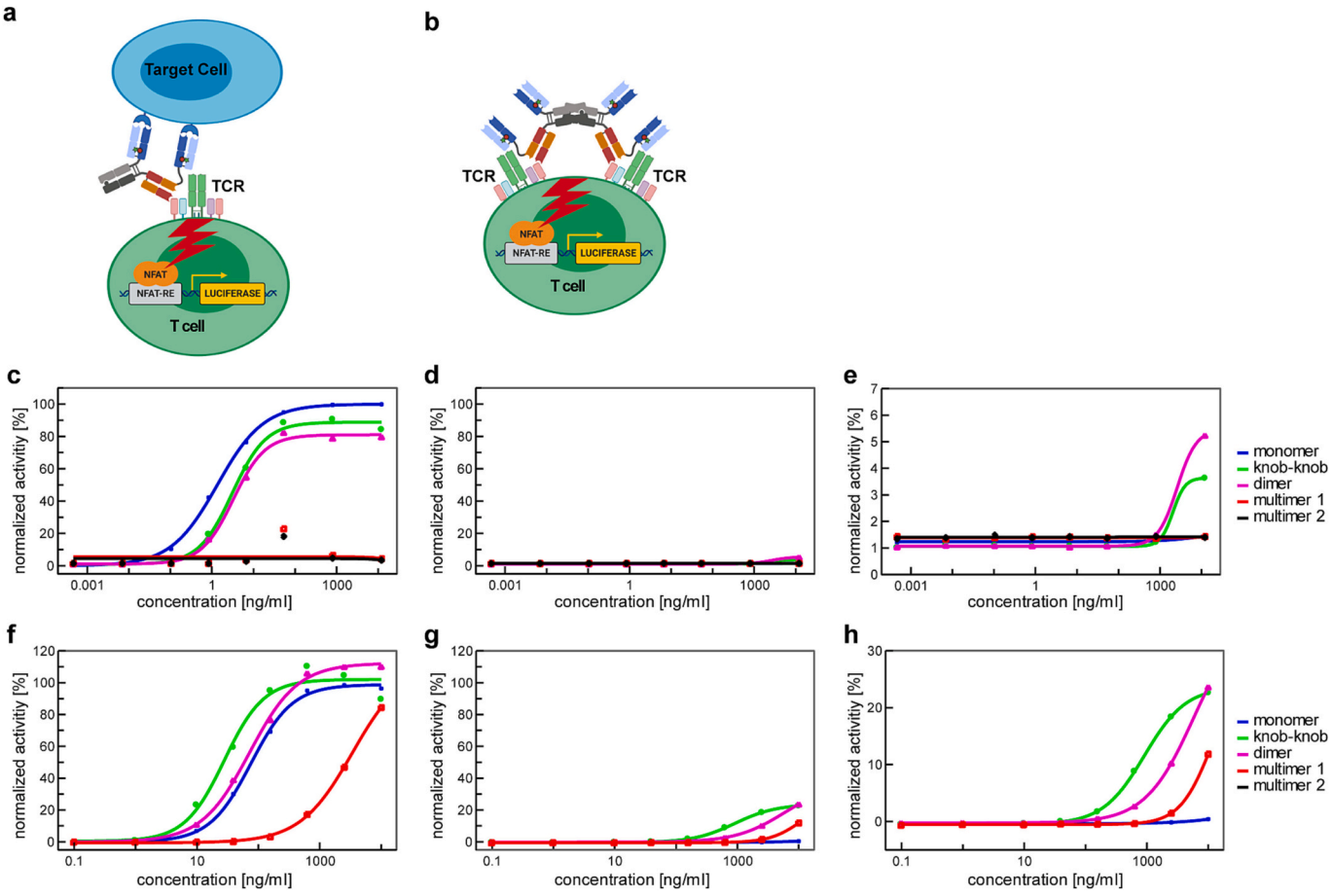

Fig. 4. Biological activity of TCB samples analyzed in a cell-based reporter gene assay. TCB monomer and HMW side-products were incubated with Jurkat NFAT-luc reporter cells in (a, c, f) the presence and (b, d, e, g, h) the absence of TAA-expressing tumor cells. The upper panels (c-e) show the data corresponding to the normalized dose-dependent activity of TAA1-TCB, while the lower panels (d-e) show similar data generated with a second TCB (TAA2-TCB). (Note: e and f are magnifications of d and g, respectively).

Interestingly, *in vitro* target-independent T cell activation has also been reported for a [1+1] TCB and its HMW side-products (Lee et al., 2019b). Similar to our observations, anti-CD3 homodimers were shown to lead to stronger activation than TCB oligomers. Overall, the functional characterization of the HMW variants by others and us confirms their T cell activation potential, and emphasizes that limiting and quantifying their levels are critical to ensure proper quality for clinical applications.

3.4. Assessment of potential safety impact of HMW species in whole blood assay enables specification setting

Toxicology studies with TAA1-TCB were conducted in cynomolgus monkeys. However, since the total amount of HMW species in the used batches was 2% or less, additional whole blood *in vitro* studies were performed in order to determine safety limits.

Exposure to TAA1-TCB induces strong cytokine release and T cell activation on its own, as expected from the mechanism of action. The potential activity of the HMW species was therefore evaluated by spiking HMW species (2.5% - 40%) on top of TAA1-TCB, while monitoring cytokine release and T cell activation. This assay design reflects the clinical situation where the monomer and its HMWs compete for binding to the same targets, and enables the identification of the HMW fraction that induces a relevant change in response. For this, a constant sub-optimal concentration of 10 pM TAA1-TCB was chosen, that allows for the detection of additive effects by the HMWs.

Spiking of up to 40% of multimer, dimer or knob-knob species did not induce any increase of T cell activation, as assessed by upregulation of CD69 on T cell subsets (Fig. 5a) and cytokine release into plasma (Fig. 5b. Data exemplary shown for IL-6. Similar data for IFNy, IL-6, IL-8, IL-10, TNFa, IL-2 and IL-1ß were obtained). Thus, with a safety margin of 8, as is common practice for this kind of NME, the data supported the specification of 5% HMWs for GMP-batch release (Kretsinger et al., 2019).

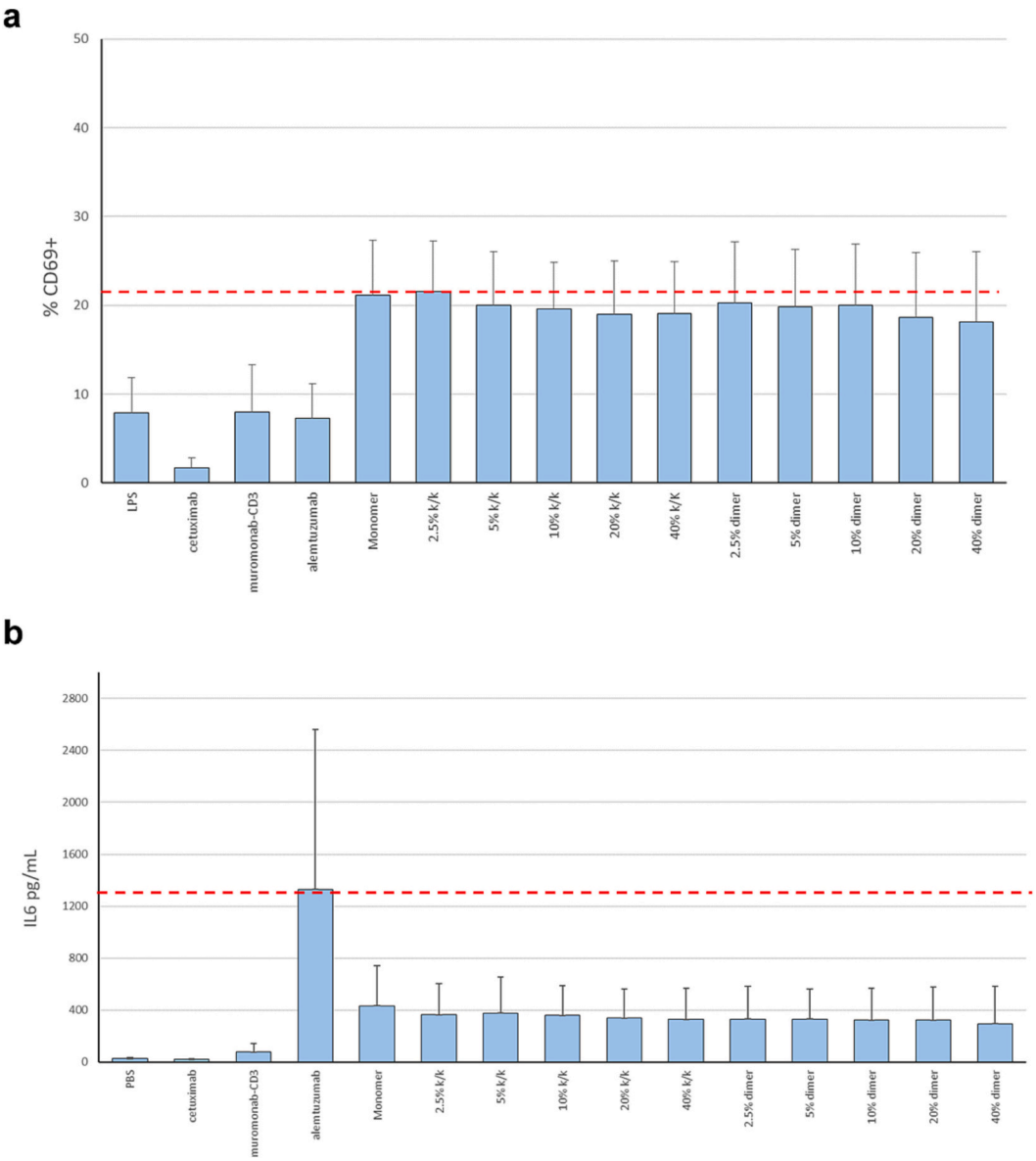

Fig. 5. Evaluation of TAA1-TCB safety profile in a whole blood assay. The effects of TAA1-TCB monomer alone and in the presence of HMW species (knob-knob and dimers) on T cell activation and cytokine release were analyzed in a spiking assay *in vitro*. Upon treatment, (a) the percentage of CD4+ T cells positive for the activation marker CD69, as well as (b) cytokine release (exemplary shown here, IL-6 secretion) were investigated. Data represents mean and standard deviation of 6 donors). PBS, cetuximab (anti-epidermal growth factor receptor antibody), muromonab-CD3 (OKT3, anti-CD3 antibody) and alemtuzumab (anti-CD52 antibody) were included as negative controls.

4. Discussion

T cell bispecifics are very potent cancer drugs which, however, bear the risk of undesired off-target T cell activation. These adverse events may be caused by the product itself but also by specific product-related impurities, which often arise during the manufacturing process. Here, we presented an integrated approach to address such side-products for [2+1] TCBs, from the proper design of the clinical lead candidate to the toxicological assessment of the remaining low amounts of impurities.

Based on our experience indicating that the incidences for knob-knob are typically lower than for hole-hole species, and on the assumption that CD3 multivalency could be a driver for target-independent T cell activation, we purposefully designed our molecule by inserting the knob mutation on the heavy chain harboring the CD3 binder. Of note, for both TAA-TCBs, no light chain mispairing was detected by mass spectrometry after the first chromatographic step (data not shown). The reported cases illustrate the manifold usefulness of isolated product-related impurities. They are indeed instrumental for guiding cell line selection, developing proper control methods, their functional characterization, and finally for their toxicological assessment, all key steps that support first-in-man studies. For this reason, we have meanwhile integrated an early supply of format-related impurities (*e.g.* knob-knob or hole-hole) to our generic technical development workflow. As exemplified here, side-products can usually be produced in a targeted manner and do not need to be isolated as a minor fraction from large amounts of the product. Depending on the technology used for generating bispecific antibodies, alternative approaches for isolating the corresponding impurities may be available. For instance, Lee et al. described a [1+1] TCB based on the "knob-into-hole" technology, where the final molecule is obtained by *in vitro* reduction and assembly of half antibodies produced by two individual cell lines. In this case, the hole-hole impurities could be isolated directly from the cell culture supernatant of the anti-CD3 half antibody producer cell line (Lee et al., 2019b).

The method developed for measuring the amount of HMW impurities present in TAA1-TCB batches relies on SEC, a well-established technology that is sensitive, precise and easy to implement, even in a GMP environment. In contrast to other approaches (Lee et al., 2019b), the method is fast and does not require specific reagents. Furthermore, since SEC is normally part of the control strategy, no additional measurements are required to control these impurities.

The functional characterization of knob-knob impurities revealed that at high drug concentrations bivalent binding to CD3 is sufficient to trigger T cell activation. While Lee et al. observed a similar behavior for another CD3-binding homodimer, a [2+2] T cell bispecific TandAb directed against CD19 (AFM11) was shown to mediate T cell activation in a strictly target-dependent manner (Reusch et al., 2015). And, similarly, Teplizumab, an anti-CD3 bivalent monospecific antibody devoid of FcγR binding, elicited only mild cytokine release syndrome in a minority of patients (Sherry et al., 2011). Therefore, the ability to activate T cells through CD3 dimerization only, without further cross-linking through target or FcγR binding, does not appear to be a general feature of these products or side-products. It is thus probable that also the CD3 epitope and/or the molecular format -and consequently the topology of the formed TCR clusters- play a significant role. Hence, functionality and safety evaluation of the corresponding impurities should be performed in a product-specific manner.

Finally, for hyperpotent HMW species, it may be necessary to reduce the specification for batch release, accordingly. Standardly, it is expected that the maximum tolerated dose will be determined by the clinical effects of cytokine release and T cell activation induced by the TAA1-TCB. However, in cases where high TCB doses are required, HMWs should be specifically considered.

The overall procedure described here constitutes a holistic approach to address product-related impurities in T cell bispecifics preparations. Although some points of this approach are specific to the utilized format, protein engineering technology and molecule mechanism of action, many aspects may be generalized to next-generation biologics where product-related impurities may be relevant for product safety or pharmaco-kinetics.

Funding details

This study and editorial support for the preparation of this manuscript is funded by Roche Pharma Research and Early Development.

CRediT authorship contribution statement

Laurent Larivière: Conceptualization, Investigation, Writing – original draft. **Julia Eva Krüger:** Methodology, Investigation. **Thomas von Hirschheydt:** Methodology, Investigation. **Tilman Schlothauer:** Methodology, Investigation. **Katharine Bray-French:** Methodology, Data curation. **Martin Bader:** Supervision. **Valeria Runza:** Writing – review & editing, Supervision.

Declaration of Competing Interest

Valeria Runza reports a relationship with Roche Diagnostics GmbH that includes: employment and equity or stocks. Laurent Lariviere reports a relationship with Roche Diagnostics GmbH that includes: employment and equity or stocks. Julia Krüger reports a relationship with Roche Diagnostics GmbH that includes: employment and equity or stocks. Tilman Schlothauer reports a relationship with Roche Diagnostics GmbH that includes: employment and equity or stocks. Martin Bader reports a relationship with Roche Diagnostics GmbH that includes: employment and equity or stocks. Katharine Bray-French reports a relationship with F. Hoffmann-La Roche AG that includes: employment and equity or stocks. Thomas von Hirschheydt reports a relationship with Roche Diagnostics GmbH that includes: employment and equity or stocks.

Data availability

The data that has been used is confidential.

Acknowledgements

We would like to express our sincere gratitude to all team members at Roche Innovation Centers Munich, Basel and Zurich who contributed to the characterization and control of product related impurities in the various T cell bispecific antibody preparations along the past years. Most especially, we thank Christian Spick, Sabine Lingke, Marcus Schmid, Harald Duerr, Oliver Ploettner, Laura Silbermann, Andrea Ritzer, and Melanie Elsner for their excellent technical support.

Appendix A. Supplementary data

Supplementary data to this article can be found online at https://doi.org/10.1016/j.ijpx.2023.100157.

References

Bacac, M., Fauti, T., Sam, J., Colombetti, S., Weinzierl, T., Ouaret, D., Bodmer, W., Lehmann, S., Hofer, T., Hosse, R.J., et al., 2016a. A novel carcinoembryonic antigen T-cell bispecific antibody (CEA TCB) for the treatment of solid tumors. Clin. Cancer Res. 22, 3286–3297.

Bacac, M., Klein, C., Umana, P., 2016b. CEA TCB, a novel head-to-tail 2:1 T cell bispecific antibody for treatment of CEA positive solid tumors. Oncoimmunology. 5 (8), e1203498.

Bacac, M., Colombetti, S., Herter, S., Sam, J., Perro, M., Chen, S., Bianchi, R., Richard, M., Schoenle, A., Nicolini, V., et al., 2018. CD20-TCB with obinutuzumab pretreatment as next-generation treatment of hematologic malignancies. Clin. Cancer Res. 24, 4785–4797.

Baeuerle, P.A., Reinhardt, C., 2009. Bispecific T-cell engaging antibodies for cancer therapy. Cancer Res. 69, 4941–4944.

Brinkmann, U., Kontermann, R., 2017. The making of bispecific antibodies. Mabs. 9, 182–212.
Carter, P., 2001. Bispecific human IgG by design. J. Immunol. Methods 248, 7–15.
Dhillon, S., 2022. Tebentafusp: first Approval. Drugs. 82 (6), 703–710.
Einsele, H., Borghaei, H., Orlowski, R., Subklewe, M., et al., 2020. The BiTE (Bispecific T-Cell engager) platform: development and future potential of a targeted immuno-oncology therapy across Tumor Types. Cancer. 126 (14), 3192–3201.
Ellerman, D., 2019. Bispecific T-cell engagers: Towards understanding variables influencing the in vitro potency and tumor selectivity and their modulation to enhance their efficacy and safety. Methods. 154, 102–117.
Elliott, J.M., Ultsch, M., Lee, J., Tong, R., Takeda, K., Spiess, C., Eigenbrot, C., Scheer, J. M., 2014. Antiparallel conformation of knob and hole aglycosylated half-antibody homodimers is mediated by a CH2-CH3 hydrophobic interaction. J. Mol. Biol. 426, 1947–1957.
Franquiz, M.J., Short, N., 2020. J. 2020. Blinatumomab for the Treatment of Adult B-Cell Acute Lymphoblastic Leukaemia: toward a New Era of Targeted Immunotherapy. Biol. Targets Ther. 14, 23–34.
Giese, G., Williams, A., Rodriguez, M., Persson, J., 2018. Bispecific antibody process development: Assembly and purification of knob and hole bispecific antibodies. Biotechnol. Prog. 34, 397–404.
Hong, P., Koza, S., Bouvier, E.S.P., 2012. Size-exclusion chromatography for the analysis of protein biotherapeutics and their aggregates. J. Liq. Chromatogr. Relat. Technol. 35, 2923–2950.
ICH Harmonised Tripartite Guideline on Quality of Biotechnological Products Q5D, 1997. Internal Conference on Harmonisation of Technical Requirements for Registration of Pharmaceuticals for Human.
ICH Harmonised Tripartite Guideline on Specifications Q6B, 1999. Internal Conference on Harmonisation of Technical Requirements for Registration of Pharmaceuticals for Humans.
ICH Harmonised Tripartite Guidelines on Pharmaceutical Development, 2009. International Conference on Harmonisation of Technical Requirements for Registration of Pharmaceuticals for Humans Q8.
Kang, C., 2022a. Mosunetuzumab: First Approval. Drugs. 82 (11), 1229–1234.
Kang, C., 2022b. Teclistamab: first Approval. Drugs. 82 (16), 1613–1619.
Klein, C., Schaefer, W., Regula, J.T., Dumontet, C., Brinkmann, U., Bacac, M., Umaña, P., 2019. Engineering therapeutic bispecific antibodies using CrossMab technology. Methods. 154, 21–31.
Kretsinger, J., Frantz, N., Hart, S.A., Kelley, W.P., Kitchen, B., Novick, S., Rellahan, B., Stranges, D., Stroop, C.J.M., Yin, P., et al., 2019. Expectations for phase-appropriate drug substance and drug product specifications for early-stage protein therapeutics. J. Pharm. Sci. 108, 1442–1452.
Kuglstatter, A., Stihle, M., Neumann, C., Muller, C., Schaefer, W., Klein, C., Benz, J., 2017. Structural differences between glycosylated, disulfide-linked heterodimeric Knob-into-Hole Fc fragment and its homodimeric Knob-Knob and Hole-Hole side products. Protein Eng. Des. Sel. 30, 649–656.
Labrijn, A.F., Meesters, J.I., de Goeij, B.E., van den Bremer, E.T., Neijssen, J., van Kampen, M.D., Strumane, K., Verploegen, S., Kundu, A., Gramer, M.J., et al., 2013. Efficient generation of stable bispecific IgG1 by controlled Fab-arm exchange. Proc. Natl. Acad. Sci. U. S. A. 110, 5145–5150.
Lalonde, M.E., Durocher, Y., 2017. Therapeutic glycoprotein production in mammalian cells. J. Biotechnol. 251, 128–140.
Lee, H.Y., et al., 2019a. Development of a bioassay to detect T-cell-activating impurities for T-cell-dependent bispecific antibodies. Sci. Rep. 9, 3900.
Lee, H.Y., Register, A., Shim, J., Contreras, E., Wu, Q., Jiang, G., 2019b. Characterization of a single reporter-gene potency assay for T-cell-dependent bispecific molecules. mAbs. 11, 1245–1253.
Lehmann, S., Perera, R., Grimm, H.P., Sam, J., Colombetti, S., Fauti, T., Fahrni, L., Schaller, T., Freimoser-Grundschober, A., Zielonka, J., et al., 2016. In vivo fluorescence imaging of the activity of CEA TCB, a novel T-cell bispecific antibody, reveals highly specific tumor targeting and fast induction of T-cell-mediated tumor killing. Clin. Cancer Res. 22, 4417–4427.
Li, Y., 2019. A brief introduction of IgG-like bispecific antibody purification: *methods* for removing product-related impurities. Protein Expr. Purif. 155, 112–119.
Regula, J.T., Imhof-Jung, S., Mølhøj, M., Benz, J., Ehler, A., Bujotzek, A., Schaefer, W., Klein, C., 2018. Variable heavy–variable light domain and Fab-arm Cross*Mabs* with charged residue exchanges to enforce correct light chain assembly. Protein Eng. Des. Sel. 31, 289–299.
Reusch, U., Duell, J., Ellwanger, K., Herbrecht, C., Knackmuss, S.H., Fucek, I., Eser, M., McAleese, F., Molkenthin, V., Gall, F.L., et al., 2015. A tetravalent bispecific TandAb (CD19/CD3), AFM11, efficiently recruits T cells for the potent lysis of CD19(+) tumor cells. mAbs. 7, 584–604.
Roberts, C.J., 2014. Therapeutic protein aggregation: Mechanisms, design, and control. Trends Biotechnol. 32, 372–380.
Sherry, N., Hagopian, W., Ludvigsson, J., Jain, S.M., Wahlen, J., Ferry, R.J., Bode, B., Aronoff, S., Holland, C., Carlin, D., et al., 2011. Teplizumab for treatment of type 1 diabetes (Protégé study): 1-year results from a randomised, placebo-controlled trial. Lancet. 2011378, 487–497.
Stecha, P., Grailer, J., Cheng Z-j, J., Hartnett, J., Fan, F., Cong, M., 2015. Abstract 5439: Development of a robust reporter-based T-cell activation assay for bispecific therapeutic antibodies in immunotherapy. Cancer Res. 75, 5439.
Trabolsi, A., Arumov, A., Schatz, J.H., 2019. T cell–activating bispecific antibodies in cancer therapy. J. Immunol. 203, 585–592.
Van Beers, M.M., Bardor, M., 2012. Minimizing immunogenicity of biopharmaceuticals by controlling critical quality attributes of proteins. Biotechnol. J. 7, 1473–1484.
Yu, L., Wang, J., 2019. T cell-redirecting bispecific antibodies in cancer immunotherapy: recent advances. J. Cancer Res. Clin. Oncol. 145, 941–956.